
UNIVERSITY
OF WOLLONGONG
AUSTRALIA

University of Wollongong
Research Online

Faculty of Engineering and Information Sciences - Papers: Part A

Faculty of Engineering and Information Sciences

2014

Effects of annealing on microstructure and microstrength of metallurgical coke

Xing Xing
University Of New South Wales, x.xing@unsw.edu.au

Guangqing Zhang
University of Wollongong, gzhang@uow.edu.au

Harold Rogers
BlueScope Steel Research

Paul Zulli
BlueScope Steel Limited

Oleg Ostrovski
University Of New South Wales

Publication Details

Xing, X., Zhang, G., Rogers, H., Zulli, P. & Ostrovski, O. (2014). Effects of annealing on microstructure and microstrength of metallurgical coke. Metallurgical and Materials Transactions B: Process Metallurgy and Materials Processing Science, 45 (1), 106-112.

Research Online is the open access institutional repository for the University of Wollongong. For further information contact the UOW Library: research-pubs@uow.edu.au

Effects of annealing on microstructure and microstrength of metallurgical coke

Abstract
Two metallurgical cokes were heat treated at 1673 K to 2273 K (1400 degrees celsius to 2000 degrees celsius) in a nitrogen atmosphere. The effect of heat treatment on the microstructure and microstrength of metallurgical cokes was characterized using X-ray diffraction, Raman spectroscopy, and ultramicroindentation. In the process of heat treatment, the microstructure of the metallurgical cokes transformed toward the graphite structure. Raman spectroscopy of reactive maceral-derived component (RMDC) and inert maceral-derived component (IMDC) indicated that the graphitisation degree of the RMDC was slightly lower than that of the IMDC in the original cokes; however graphitisation of the RMDC progressed faster than that of the IMDC during annealing, and became significantly higher after annealing at 2273 K (2000 degrees celsius). The microstrength of cokes was significantly degraded in the process of heat treatment. The microstrength of the RMDC was lower, and of its deterioration caused by heat treatment was more severe than IMDC. The degradation of the microstrength of cokes was attributed to their increased graphitisation degree during the heat treatment.

Keywords
microstructure, microstrength, metallurgical, effects, coke, annealing

Disciplines
Engineering | Science and Technology Studies

Publication Details
Xing, X., Zhang, G., Rogers, H., Zulli, P. & Ostrovski, O. (2014). Effects of annealing on microstructure and microstrength of metallurgical coke. Metallurgical and Materials Transactions B: Process Metallurgy and Materials Processing Science, 45 (1), 106-112.

This journal article is available at Research Online: http://ro.uow.edu.au/eispapers/2100

Effects of Annealing on Microstructure and Microstrength of Metallurgical Coke

XING XING, GUANGQING ZHANG, HAROLD ROGERS, PAUL ZULLI, and OLEG OSTROVSKI

Two metallurgical cokes were heat treated at 1673 K to 2273 K (1400 °C to 2000 °C) in a nitrogen atmosphere. The effect of heat treatment on the microstructure and microstrength of metallurgical cokes was characterized using X-ray diffraction, Raman spectroscopy, and ultra-microindentation. In the process of heat treatment, the microstructure of the metallurgical cokes transformed toward the graphite structure. Raman spectroscopy of reactive maceral-derived component (RMDC) and inert maceral-derived component (IMDC) indicated that the graphitisation degree of the RMDC was slightly lower than that of the IMDC in the original cokes; however graphitisation of the RMDC progressed faster than that of the IMDC during annealing, and became significantly higher after annealing at 2273 K (2000 °C). The microstrength of cokes was significantly degraded in the process of heat treatment. The microstrength of the RMDC was lower, and of its deterioration caused by heat treatment was more severe than IMDC. The degradation of the microstrength of cokes was attributed to their increased graphitisation degree during the heat treatment.

DOI: 10.1007/s11663-013-0002-y
© The Minerals, Metals & Materials Society and ASM International 2013

I. INTRODUCTION

METALLURGICAL coke is a major material used in blast furnace (BF) ironmaking. In BF ironmaking, which is a shaft furnace-based process, coke is used as both a reductant and fuel. However, the structural support to the burden column is the most significant function that coke fulfils in the BF as the other roles of coke can be substituted to some extent with other carbonaceous materials, such as pulverized coal for tuyere injection. Therefore, coke with good mechanical strength is required to ensure good permeability of the liquid, powder, and gas phases flowing through the burden in the blast furnace.

The mechanical strength of coke is much higher than the load to which coke is subjected in the blast furnace. However, the coke collected from the lower region of the furnace shows evidence of degradation, such as lump-size decrease and microtextural changes. Previous studies on parameters determining mechanical strength of metallurgical cokes suggested that the mechanical strength of coke was affected by the pore structure and the microstrength of coke wall components structure.[1–6].

Microstructure of carbonaceous materials has been extensively studied using X-ray diffraction (XRD) and Raman spectroscopy.[7–18] Heating of cokes was shown to have a significant impact on the growth of crystallite size, L_c, by demonstrating the correlation between crystallite size and annealing temperature.[15,18,19] Correspondingly, the proportion of graphite-like structure increased during the thermal heating process.[10]

Microstrength of carbonaceous materials has been investigated by ultra-microindentation,[5,6,20–23] with a principal focus on the effect of coking condition and reaction on the microstrength of the cokes. However, little has been reported on the effect of annealing on the microstrength of metallurgical cokes, especially in the temperature range found in the lower region of the blast furnace. The mechanism of the change in the microstrength of metallurgical cokes upon heating is still unclear.

The aim of this paper is to study the effect of heat treatment under inert conditions on the microstructure and microstrength of metallurgical coke in the temperature range of 1673 K to 2273 K (1400 °C to 2000 °C), and develop an understanding of the mechanism of change in microstrength during heat treatment.

II. EXPERIMENTAL

A. *Materials*

Two metallurgical cokes, Coke A and Coke C, studied in this work. One coke is from a commercial BF operation and the second was produced in a pilot coke oven. Proximate analysis of cokes is shown in Table I.

XING XING, Postdoctoral Fellow and OLEG OSTROVSKI, Professor, are with the School of Materials Science and Engineering, University of New South Wales, Sydney, NSW 2052, Australia. Contact e-mail: x.xing@unsw.edu.au GUANGQING ZHANG, Lecturer, is with the School of Mechanical, Materials & Mechatronic Engineering, University of Wollongong, Wollongong, NSW 2522, Australia. HAROLD ROGERS, Research Associate, and PAUL ZULLI, Research Manager, are with the BlueScope Steel, Port Kembla, NSW 2505 Australia.

Manuscript submitted September 23, 2013.
Article published online December 3, 2013.

B. *Heat Treatment*

Approximately 200 g of coke with a particle size of 19 to 21 mm was heat treated in a graphite furnace under nitrogen atmosphere for 2 h at temperatures of 1673 K, 1873 K, 2073 K, and 2273 K (1400 °C, 1600 °C, 1800 °C, and 2000 °C). The heating rate was fixed at 25 K min^{-1} (25 °C min^{-1}). The samples were contained in a graphite crucible, into which 1 L min^{-1} of nitrogen (99.99 pct) was continuously blown through a graphite ducting tube attached to the bottom of the crucible. A type B thermocouple was inserted through the gas ducting tube with the tip located at the center of the coke bed. Heat treatment was counted from the time when the furnace temperature reached the designated level.

C. *Microstructure of Carbonaceous Materials*

1. *X-ray diffraction of carbonaceous materials*

XRD spectra of powdered samples were obtained using Philips X'Pert multipurpose X-ray diffraction system (MPD). Cu K_α radiation (45 kV, 40 mA) was used as the X-ray source. Samples were scanned with 2θ in the range of 10 to 50 deg with a step size of 0.02 deg and 0.6 seconds scanning time at each step.

The crystallite size, $\boldsymbol{L_c}$, or stack height and interlayer spacing between aromatic planes of carbon crystallites, $\boldsymbol{d_{002}}$, (Figure 1) were calculated using the Scherrer equation[24] and Bragg's Law.[25] The wavelength of incident X-ray for Cu K_α radiation in this study was 1.5409 Å.

2. *Raman spectroscopy of carbonaceous materials*

Carbonaceous materials were also analyzed using a Renishaw inVia Raman microscope with a 514 nm excitation wavelength. The beam size was 1.5 to 2 μm, which allowed analysis of inert maceral-derived component (IMDC) and reactive maceral-derived component (RMDC) separately. Raman spectra were scanned from 900 to 1900 cm^{-1} with 25 mW laser power for an exposure time of 15 seconds. The appearance of IMDC and RMDC under plane reflected light with air gap objective is shown in Figure 2. At least ten measurements in different zones were taken for each type of microtexture. Highly ordered pyrolytic graphite (HOPG) was also analysed by Raman spectroscope as a reference material with a high degree of graphitisation.

Figure 3 shows a typical first order Raman profile of RMDC texture of metallurgical cokes annealed at high temperature. The Raman spectrum consists of two apparent peaks, overlapped G* and D* bands centered at around 1600 and 1360 cm^{-1}, respectively. It was reported that both G* and D* bands became sharper with increasing annealing temperature, and the G* band split into two peaks centered at 1580 and 1620 cm^{-1}, respectively after annealing at 2073 K (1800 °C).[9,26] In previous investigations, different curve fitting methods of G* and D* bands were attempted; Ferrari and Robertson[27] focused only on G* and D* peaks at 1600 and 1350 cm^{-1}. Dong *et al.*[7] fitted the G* and D* bands with G, D, R_1, and R_2 peaks. Sheng[28] and Kawakami *et al.*[10] further separated G peak into two peaks centered at around 1580 and 1620 cm^{-1}, respectively. Li *et al.*[29] deconvoluted G* and D* bands more finely into ten individual peaks.

In the present work, overlapped G* and D* bands were deconvoluted into five peaks with Lorentzian band fitting: G, D, D′, R_1, and R_2 (Figure 3). The G peak represents the Raman scattering from the inner graphitic plane which arises from E_{2g} (1580 cm^{-1}) peak.[7] The E_{2g} peak is attributed to the stretching vibration mode in the aromatic layer of the graphite crystallite.[14,27,28,30] The D′ peak appears near the high frequency edge of the vibrational states of the carbon lattice.[31] The D peak, which represents the disordered carbon, is due to the breathing modes of A_{1g} symmetry involving phonons near the K zone boundary which is active only in the presence of disorder.[14,27] R_1 and R_2 peaks are assigned to the so-called turbostratic or random structure, which has an intermediate structure between graphite and an amorphous state.[17,32,33]

Based on the above interpretation of Raman bands, the G fraction which characterizes coke graphitisation was calculated as ratio of area under the G peak to the total area.[7]

Table I. Proximate Analysis of Coke Samples (Wt Pct Air-Dried Basis)

	Coke A	Coke C
M_{ad}	0.39	0.51
V_{ad}	1.39	1.53
A_{ad}	11.92	12.08

M_{ad} is moisture in the air-dry sample. V_{ad} is volatile matter in the air-dry sample. A_{ad} is ash in the air-dry sample.

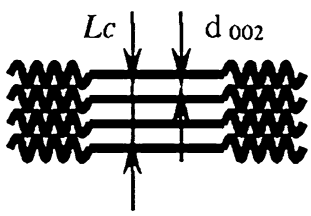

Fig. 1—Single carbon crystallite.

D. *Microstrength of Carbonaceous Materials*

Microstrength of each coke was determined using a UMIS2000 ultra-microindentation system. Earlier indentation studies on metallurgical cokes showed that using a Berkovich indenter with a centerline-to-face angle of 65.27 deg, there was very little plastic deformation with no residual indenter impress after full load, and no crack formation.[5,6] Therefore a sharper cube corner indenter, with a centerline-to-face angle of 35.26 deg, was used when a residual impression and measurable radial cracks were needed. Indentations were made on the polished surface of resin-mounted samples with an appropriate indenter.

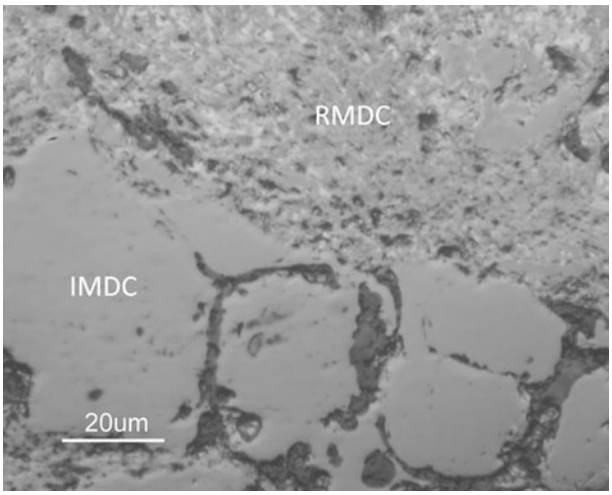

Fig. 2—Inert maceral-derived component (IMDC) and reactive maceral-derived component (RMDC) of Coke A.

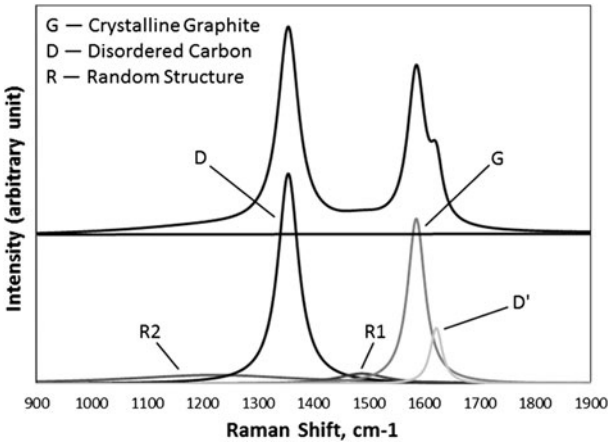

Fig. 3—Typical Raman profile of inert maceral-derived component (IMDC) or reactive maceral-derived component (RMDC) for metallurgical cokes.

1. *Hardness and Young's modulus*

A three-sided Berkovich indenter was applied to determine the hardness, H, and Young's modulus, E. A load of 100 mN was applied, and ten measurements for each type of coke microtexture and HOPG were carried out across several sample lumps. Hardness and Young's modulus were determined according to the loading–unloading curve generated by increasing applied load and measuring the depth of penetration of the diamond indenter.

The hardness, H, and Young's modulus, E, were calculated according to the method developed by Oliver and Pharr.[34]

2. *Fracture toughness*

The measurement of fracture toughness relies upon the optical microscope measurement of the crack length of the residual impression formed after indentation. Fracture toughness of the two coke microtextures and HOPG was determined using 200 and 50 mN loads, respectively, with cube corner indenter. Determinations of fracture toughness were located at ten different locations and crack lengths of residual impression after full unload were measured from the images obtained by the digital camera linked to the microscope of the UMIS. The fracture toughness $\boldsymbol{K_{1c}}$ was calculated using experimental hardness, Young's modulus, length of cracks, and geometry of the applied indenter.[35]

III. RESULTS AND DISCUSSION

A. *Effect of Heat Treatment on Microstructure of the Metallurgical Cokes*

1. *XRD analysis*

The XRD spectra with profiles of 002 carbon peak of original Cokes A and C, and annealed at different temperatures are presented in Figure 4. The peaks at 26.6 and 20.8 deg in original samples were assigned to quartz in the coke ash; they were substantially removed in annealing above 1673 K (1400 °C). The shape of the 002 carbon peaks is used as a qualitative indication of the graphitisation degree of metallurgical cokes; coke samples with shaper 002 peaks have a larger crystal size and greater degree of graphitisation. The comparison of XRD patterns of coke annealed at different temperatures shows that the 002 carbon peak became sharper with increasing annealing temperature.

The effects of annealing on the carbon crystallite size $\boldsymbol{L_c}$ and interlayer spacing $\boldsymbol{d_{002}}$ cokes subjected to different annealing temperature are presented in Figures 5 and 6, respectively. The crystallite size $\boldsymbol{L_c}$ of both cokes increased significantly with increasing heat treatment temperature; the increase became more prominent at high temperatures. The crystallite size $\boldsymbol{L_c}$ of original Coke C was slightly lower than that of original Coke A; however in the process of annealing, the crystallite size of Coke C grew faster than that of Coke A. After heat treatment at 2273 K (2000 °C), the crystallite size $\boldsymbol{L_c}$ of Coke C was 20 pct higher than Coke A.

Interlayer spacing $\boldsymbol{d_{002}}$ was also strongly affected by the annealing temperature. Increasing annealing temperature resulted in a denser structure and decreased $\boldsymbol{d_{002}}$ value. However, the minimum $\boldsymbol{d_{002}}$ value among all coke samples was higher than that of HOPG (3.36 Å).

2. *Raman spectroscopy analysis*

The Raman spectra of RMDC microtexture of Coke A annealed at different temperatures are shown in Figure 7. This figure also includes Raman spectrum of HOPG. The Raman spectrum of original coke contained two overlapped G* and D* bands centered at around 1600 and 1360 cm^{-1}, respectively. Both of these bands became sharper with increasing annealing temperature; G* band split into G and D′ peaks after heat treatment at 2073 K (1800 °C), and the D′ peak became more evident after annealing at 2273 K (2000 °C). Raman spectrum of HOPG presented three individual peaks centered at 1355, 1580, and 1620 cm^{-1}. Comparison of the Raman spectra of metallurgical coke and HOPG indicates that the structure of metallurgical coke transformed towards HOPG with increasing annealing temperature.

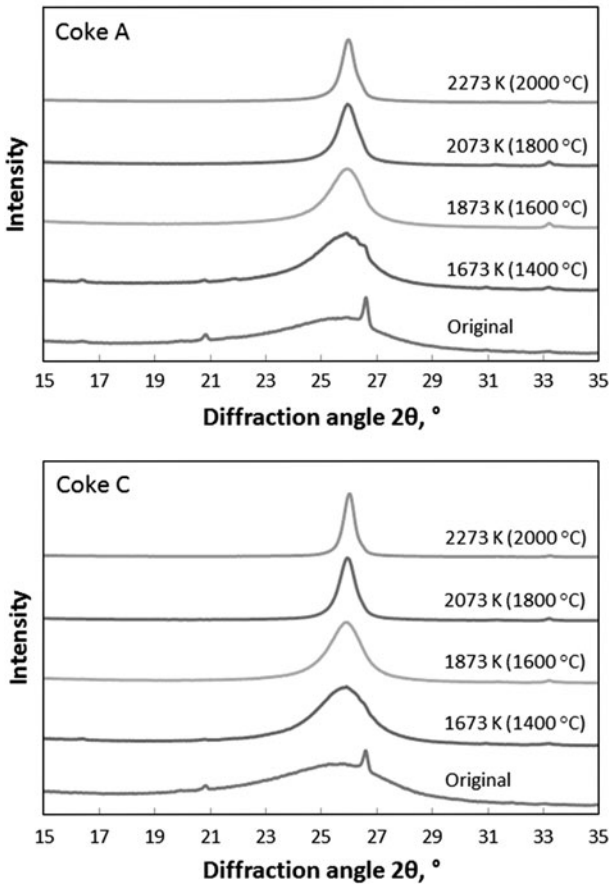

Fig. 4—Profiles of 002 carbon peaks in XRD spectra of original Cokes A and C, and after annealing at different temperatures.

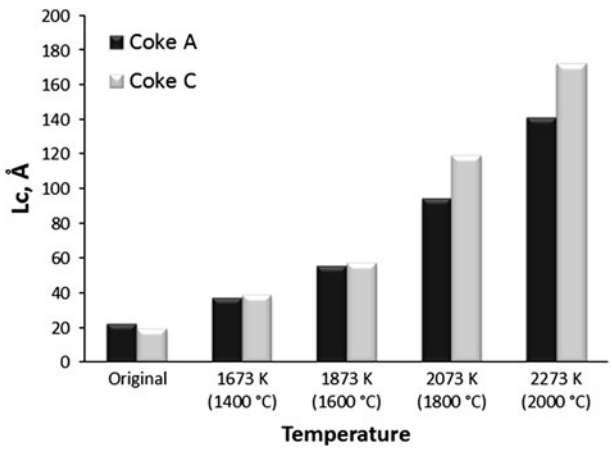

Fig. 5—Crystallite sizes (L_c) of Coke A and Coke C annealed at different temperatures.

The Raman spectra were deconvoluted into G, D, D′, R_1, and R_2 peaks as described previously with Lorentzian band fitting, and G fraction of Coke A, Coke C, and HOPG was calculated. The G fractions of Coke A and Coke C heat treated at different temperatures are presented in Figure 8. G fraction of all microtextural types in the tested coke samples increased as annealing temperature

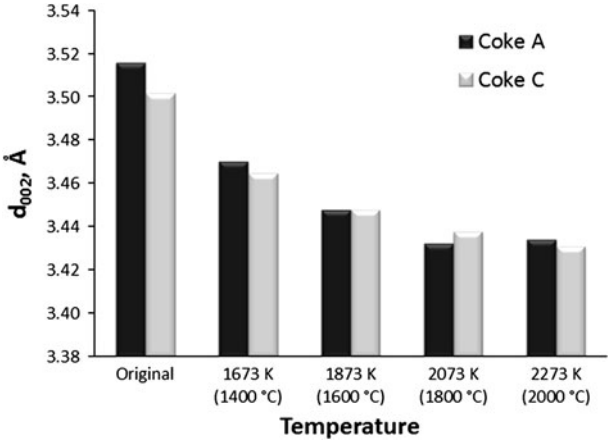

Fig. 6—Interlayer spacing (d_{002}) of Coke A and Coke C annealed at different temperatures.

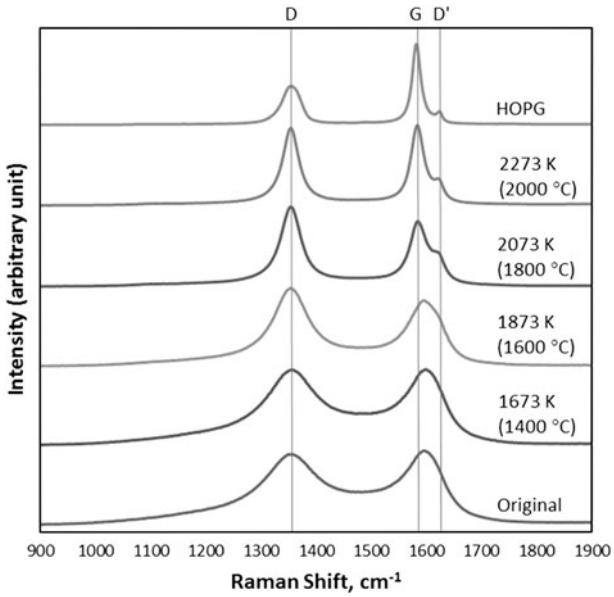

Fig. 7—Raman spectra of RMDC of Coke A annealed at different temperatures and HOPG.

increased which indicates that the proportion of graphite structure in cokes increased in the process of thermal annealing. The G fraction of tested HOPG was approximately 52 pct which was higher than the G fraction of cokes annealed at 2273 K (2000 °C).

In both coke samples, the G fraction of the RMDC of original coke samples was slightly lower than that of the IMDC. However, the G fraction of the RMDC and IMDC reached the same level after heat treatment at 1673 K (1400 °C); with further increase in the annealing temperature the G fraction of the RMDC became higher than that of the IMDC, and the difference became larger with further increase in the heat treatment temperature. These changes in G fraction of the RMDC and IMDC indicate that the graphitisation degree and the effect of temperature on it were higher for the RMDC than for the IMDC for both cokes.

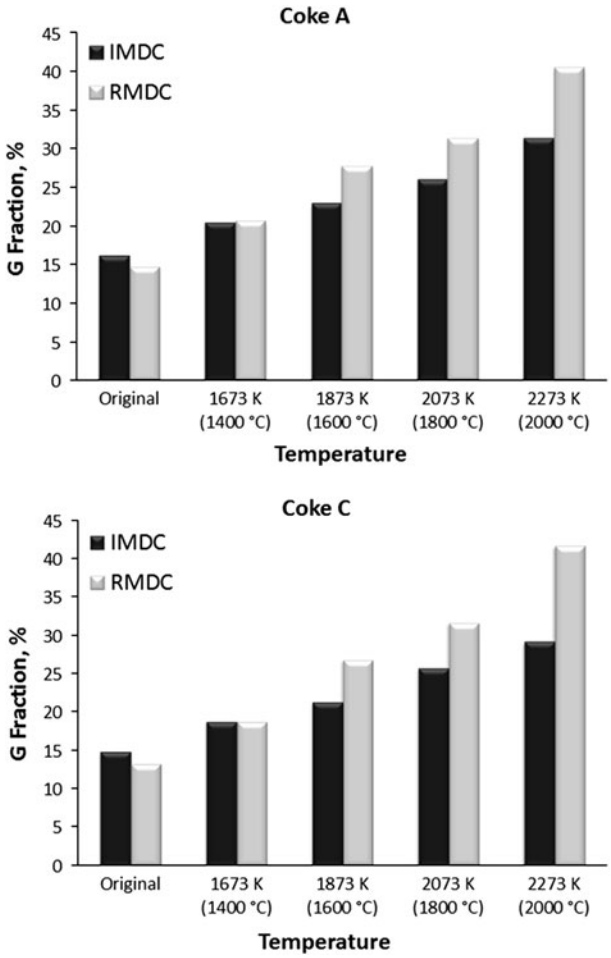

Fig. 8—G fraction of Coke A and Coke C annealed at different temperatures.

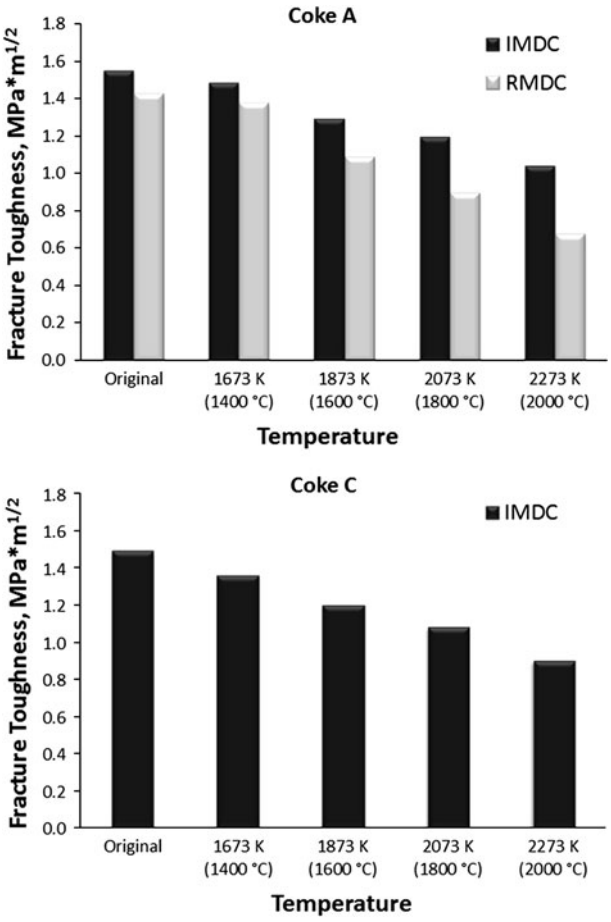

Fig. 9—Fracture toughness of original coke samples and after annealing at different temperatures.

B. *Effect of Heat Treatment on the Microstrength of the Metallurgical Cokes*

The fracture toughness of coke samples and HOPG was calculated using experimental data on hardness and Young's modulus, and the measurement of the crack length of the residual impression after indentation. The fracture toughness of the original cokes and after annealing at different temperatures is presented in Figure 9. The crack length of residual impression after microindentation of RMDC in Coke C was difficult to measure as this microtexture is dominated by coarse mosaic and foliate microtexture. Therefore, the fracture toughness of Coke C was studied only for IMDC.

Fracture toughness of IMDC in the original cokes was 1.5 to 1.6 MPa $m^{1/2}$. Heat treatment of coke samples in the temperature range of 1673 K to 2273 K (1400 °C to 2000 °C) degraded the fracture toughness of both Coke A and Coke C. After annealing at 2273 K (2000 °C), the fracture toughness of the IMDC of Coke C was 0.9 MPa $m^{1/2}$ which was 13.5 pct lower than that of Coke A. The fracture toughness of RMDC of original Coke A was slightly lower than that of IMDC, and the deterioration of RMDC caused by heat treatment was more severe than IMDC. After heat treatment at 2273 K (2000 °C), the fracture toughness of RMDC was 0.7 MPa $m^{1/2}$, which is approximately 34.6 pct lower than that of IMDC. Compared with metallurgical cokes, HOPG had a fracture toughness of 0.32 MPa $m^{1/2}$, which was 67 pct lower than IMDC and 53 pct lower than RMDC of metallurgical cokes.

C. *Correlation of Microstructure and Microstrength*

Crystallite size, L_c, and G fraction of graphite structure in carbonaceous material are used as an indication of graphitisation degree of the metallurgical cokes. During heat treatment in the temperature range of 1673 K to 2273 K (1400 °C to 2000 °C), L_c parameter and G fraction increased significantly for all samples tested. The Raman spectrum of coke annealed at 2273 K (2000 °C) had a similar shape to the Raman spectrum of HOPG. These parameters indicate that the graphitisation degree increased and the carbon structure of coke samples transformed towards the graphite structure in the process of heat treatment.

The microstrength of cokes, represented by fracture toughness, degraded during annealing at 1673 K to 2273 K (1400 °C to 2000 °C). Correlation of microstructure and microstrength of cokes was tested by plotting fracture toughness against G fraction. Correlation between the G fractions and fracture toughness for

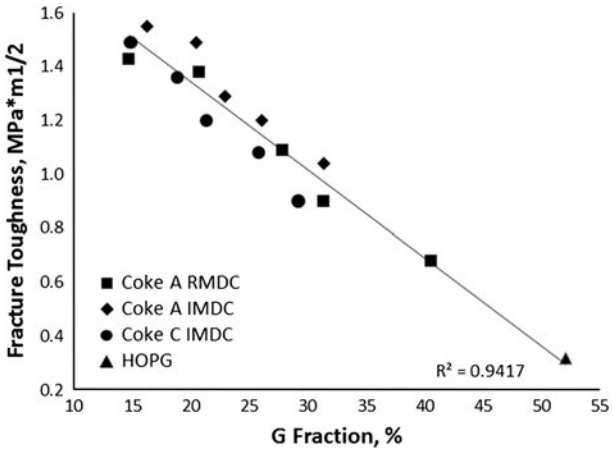

Fig. 10—Correlation of G fraction and fracture toughness of metallurgical cokes and HOPG.

RMDC and IMDC of Coke A and IMDC of Coke C is shown in Figure 10. This plot also includes the G fraction and fracture toughness of HOPG.

The HOPG had the highest graphitisation degree and lowest fracture toughness; the fracture toughness of RMDC and IMDC of both cokes decreased with increasing G fraction; obviously, the coke matrix became weaker when the carbon structure transformed towards the graphite structure. This can be explained by the carbon structure model which describes the structure of the non-graphitic carbon as a strong system of cross-lined crystallites and the structure of graphite as parallel orientated crystallites.[36] Upon the heat treatment in the temperature range of 1673 K to 2273 K (1400 °C to 2000 °C), the microstructure of cokes transformed from a non-graphitic structure towards a graphitic structure; during this process, the cross-link structure was broken and the crystallites rearranged to form parallel structure, which has a weaker resistance to fracture.

IV. CONCLUSIONS

The effect of heat treatment in the temperature range of 1673 K to 2273 K (1400 °C to 2000 °C) on the microstructure and microstrength of metallurgical cokes was studied using XRD, Raman spectroscopy, and ultra-microindentation. The major findings are

1. In the process of heat treatment, the microstructure of the metallurgical cokes transformed towards a graphite-like structure. The graphitization degree of RMDC was slightly lower than that of IMDC in the original coke samples; however, the graphitisation degree of RMDC increased more rapidly with increasing temperature above 1673 K (1400 °C) and became significantly higher than that of IMDC after the heat treatment.
2. Heat treatment in the temperature range of 1673 K to 2273 K (1400 °C to 2000 °C) significantly degraded the fracture toughness of metallurgical cokes. Fracture toughness of RMDC was lower than that of IMDC, and the effect of heat treatment on RMDC was greater.
3. The reduction in the microstrength of metallurgical cokes was attributed to the transformation of carbon structure from non-graphite to graphite microstructure during the heat treatment.

ACKNOWLEDGMENTS

This project was supported by BlueScope Steel, BHP Billiton, and Australian Research Council (ARC Linkage Project LP130100701).

REFERENCES

1. J.W. Patrick and A. Walker: *Carbon*, 1989, vol. 27 (1), pp. 117–23.
2. M.G.K. Grant, A.C.D. Chaklader, and J.T. Price: *Fuel*, 1991, vol. 70 (2), pp. 181–88.
3. H. Sato, J.W. Patrick, and A. Walker: *Fuel*, 1998, vol. 77 (11), pp. 1203–08.
4. Y. Kubota, S. Nomura, T. Arima, and K. Kato: *ISIJ Int*., 2011, vol. 51 (11), pp. 1800–08.
5. N. Andriopoulos, C.E. Loo, R. Dukino, and S.J. McGuire: *ISIJ Int*., 2003, vol. 43 (10), pp. 1528–37.
6. X. Xing, G. Zhang, M. Dell'Amico, G. Ciezki, Q. Meng, and O. Ostrovski: *Metall. Mater. Trans. B*, 2013, vol. 44, pp. 870–77.
7. S. Dong, N. Paterson, S.G. Kazarian, D.R. Dugwell, and R. Kandiyoti: *Energy Fuels*, 2007, vol. 21 (6), pp. 3446–54.
8. T.W. Zerda, A. John, and K. Chmura: *Fuel*, 1981, vol. 60 (5), pp. 375–78.
9. M. Kawakami, T. Karato, and T. Takenaka: *ISIJ Int*., 2005, vol. 45 (7), pp. 1027–34.
10. M. Kawakami, H. Kanba, K. Sato, T. Takenaka, S. Gupta, R. Chandratilleke, and V. Sahajwalla: *ISIJ Int*., 2006, vol. 46 (8), pp. 1165–70.
11. A. Guedes, B. Valentim, A.C. Prieto, S. Rodrigues, and F. Noronha: *Int. J. Coal Geol*., 2010, vol. 83 (4), pp. 415–422.
12. T. Gruber, T.W. Zerda, and M. Gerspacher: *Carbon*, 1994, vol. 32 (7), pp. 1377–82.
13. A. Cuesta, P. Dhamelincourt, J. Laureyns, A. Martinezalonso, and J.M.D. Tascon: *Carbon*, 1994, vol. 32 (8), pp. 1523–32.
14. F. Tuinstra and J.L. Koenig: *J. Chem. Phys*., 1970, vol. 53 (3), pp. 1126–30.
15. L. Lu, V. Sahajwalla, and D. Harris: *Energy Fuels*, 2000, vol. 14 (4), pp. 869–876.
16. M.A. Short and P.L. Walker: *Carbon*, 1963, vol. 1 (1), pp. 3–9.
17. L. Lu, V. Sahajwalla, C. Kong, and D. Harris: *Carbon*, 2001, vol. 39 (12), pp. 1821–33.
18. S. Gupta, V. Sahajwalla, J. Burgo, P. Chaubal, and T. Youmans: *Metall. Mater. Trans. B*, 2005, vol. 36B, pp. 385–94.
19. J.V. Dubrawski and W.W. Gill: *Ironmak. Steelmak*., 1984, vol. 11 (1), pp. 7–16.
20. D.T. Marx and L. Riester: *Carbon*, 1999, vol. 37 (11), pp. 1679–84.
21. O. Tomoki, U. Kenta, M. Yoshio, A. Hideyuki, M. Takatoshi, U. Takatoshi, and F. Koichi: *Tetsu to Hagane*, 2006, vol. 92 (3), pp. 171–76.
22. J.S. Fielda and M.V. Swain: *Carbon*, 1996, vol. 34 (11), pp. 1357–66.
23. Y. Yamazaki, K. Hiraki, T. Kanai, X. Zhang, Y. Matsushita, M. Shoji, H. Aoki, and T. Miura: *J. Therm. Sci. Technol*., 2011, vol. 6, pp. 278–88.
24. T.F. Yen, J.G. Erdman, and S.S. Pollack: *Anal. Chem*., 1961, vol. 33, pp. 1587–94.
25. C. Suryanarayana and M.G. Norton: *X-Ray Diffraction: A Practical Approach*, Plenum Press, New York, NY, 1998, p. 50.
26. R. Kostecki, T. Tran, X. Song, K. Kinoshita, and F. McLarnon: *J. Electrochem. Soc*., 1997, vol. 144 (9), pp. 3111–17.
27. A.C. Ferrari and J. Robertson: *Phys. Rev. B*, 2000, vol. 61 (20), pp. 14095–107.
28. C. Sheng: *Fuel*, 2007, vol. 86 (15), pp. 2316–24.

29. X. Li, J. Hayashi, and C. Li: *Fuel*, 2006, vol. 85 (12–13), pp. 1700–07.
30. J. Van Doorn, M.A. Vuurman, P.J.J. Tromp, D.J. Stufkens, and J.A. Moulijn: *Fuel Process. Technol.*, 1990, vol. 24, pp. 407–13.
31. R.J. Nemanich and S.A. Solin: *Phys. Rev. B*, 1979, vol. 20 (2), pp. 392–401.
32. A.C. Ferrari, B. Kleinsorge, G. Adamopoulos, J. Robertson, W.I. Milne, V. Stolojan, L.M. Brown, A. LiBassi, and B.K. Tanner: *J. Non Cryst. Solids*, 2000, vol. 266, pp. 765–68.
33. A.C. Ferrari and J. Robertson: *Phys. Rev. B*, 2001, vol. 64 (7), pp. 1–13.
34. W.C. Oliver and G.M. Pharr: *J. Mater. Res.*, 1992, vol. 7 (6), pp. 1564–83.
35. A.C. Fischer-Cripps: *The IBIS Handbook of Nanoindentation*, Fischer-Cripps Laboratories, Forestville, NSW, 2005.
36. R.E. Franklin: *Proc. R. Soc. Lond. A*, 1097, vol. 1951 (209), pp. 196–218.